J. Membrane Biol. 193, 215–227 (2003)
DOI: 10.1007/s00232-003-2020-1

The Journal of
Membrane
Biology



# Effects of the Enantiomers of BayK 8644 on the Charge Movement of L-type Ca Channels in Guinea-pig Ventricular Myocytes

**P. Artigas[1], G. Ferreira[2], N. Reyes[2], G. Brum[2], G. Pizarro[1,2]**
Laboratorio de Biofísica del Músculo, [1]Facultad de Ciencias and [2]Facultad de Medicina, Universidad de la República, Montevideo, Uruguay

Received: 8 July 2002/Revised: 3 March 2003

**Abstract.** The effects of the agonist enantiomer S(−)Bay K 8644 on gating charge of L-type Ca channels were studied in single ventricular myocytes. From a holding potential ($V_h$) of −40 mV, saturating (250 nM) S(−)Bay K shifted the half-distribution voltage of the activation charge (*Q1*) *vs.* *V* curve −7.5 ± 0.8 mV, almost identical to the shift produced in the Ba conductance *vs.* *V* curve (−7.7 ± 2 mV). The maximum *Q1* was reduced by 1.7 ± 0.2 nC/μF, whereas *Q2* (charge moved in inactivated channels) was increased in a similar amount (1.4 ± 0.4 nC/μF). The steady-state availability curves for *Q1*, *Q2*, and Ba current showed almost identical negative shifts of −14.8 ± 1.7 mV, −18.6 ± 5.8 mV, and −15.2 ± 2.7 mV, respectively. The effects of the antagonist enantiomer R(+)BayK 8644 were also studied, the *Q1* *vs.* *V* curve was not significantly shifted, but $Q1_{max}$ ($V_h$ = −40 mV) was reduced and the *Q1* availability curve shifted by −24.6 ± 1.2 mV. We concluded that: a) the left shift in the *Q1* *vs.* *V* activation curve produced by S(−)BayK is a purely agonistic effect; b) S(−)BayK induced a significantly larger negative shift in the availability curve than in the *Q1* *vs.* *V* relation, consistent with a direct promotion of inactivation; c) as expected for a more potent antagonist, R(+)Bay K induced a significantly larger negative shift in the availability curve than did S(−) Bay K.

**Key words:** L-type Ca channel — Dihydropyridines — Gating currents — Charge movement — Cardiac myocytes — Voltage dependent inactivation

## Introduction

1,4-dihydropyridines (DHP), which include some widely used anti-hypertensive agents, are specific modifiers of voltage gated L-type calcium channels (VLCC) affecting their voltage-dependent transitions. Some DHP compounds, like nifedipine or R(+)Bay K 8644, are called antagonists because they promote voltage-dependent inactivation and block of VLCC (Bean, 1984, Sanguinetti & Kass, 1984), while others, like S(−)Bay K 8644 or Sandoz + 202-791, increase L-type Ca currents, by increasing the open probability ($P_o$) and shifting the *I-V* curve towards more negative potentials (for review, *see* Mc Donald et al., 1994) and are consequently called agonists. Interestingly, along with the increase in $P_o$, agonistic DHPs also increase the rate of current inactivation (Kass, 1987; Reuter et al., 1988; Kamp, Sanguinetti and Miller, 1989). This antagonist-like effect of the agonistic DHP is not well understood; it has been described as promotion of voltage-dependent inactivation (Kamp et al., 1989), or as enhanced current-dependent inactivation (even when Ba was the charge carrier, Markwardt & Nilius, 1988).

To gain insight on the dual effect of S(−)BayK, we studied its effects on VLCC gating currents that report the voltage-dependent conformational changes associated with the movement of charges or dipoles in the voltage sensor of the VLCC protein. Brief depolarizing pulses move the same amount of charge in the ON (reflecting activation) and OFF (representing deactivation) transients following the transition of the channels through resting (closed) state(s) and active (open) state(s). The charge *vs.* voltage (*Q* *vs.* *V*) curve for these activating-deactivating transitions is well described by a Boltzmann distribution centered at ~0 mV (Bean & Rios, 1989). During longer depolarizing pulses the channels

*Correspondence to:* G. Pizarro; email: gpizarro@fmed.edu.uy

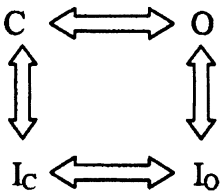


**Scheme 1.**

transit from the active state(s) to the inactivated state(s), resulting in voltage-dependent inactivation. As a consequence of inactivation, the *Q vs. V* distribution is shifted towards more negative potentials (centered at $\sim -90$ mV) resulting in an apparent immobilization of the charge in the OFF direction of the pulses. This type of voltage-dependent inactivation seems to be rather ubiquitous, and has been described in Na channels (Bezanilla, Taylor & Fernandez, 1982), in the voltage sensor of excitation contraction coupling of skeletal muscle (Brum & Ríos, 1987) and in VLCC (Shirokov et al., 1992). The simplest representation of this mechanism is presented in Scheme 1 where horizontal transitions move charge while the vertical transitions are intrinsically voltage-independent (*see* Appendix for a more detailed description). In this paper, we will refer to the charge that moves between non-inactivated channels ($C \leftrightarrow O$) as charge 1 ($Q1$) while the charge due to transitions between inactivated channels ($I_c \leftrightarrow I_o$), which occur at very negative potentials, will be called charge 2 ($Q2$).

Three previous reports of the effects of S(−)Bay on VLCC gating currents have demonstrated that this drug facilitates voltage-dependent activation of VLCC (Josephson & Sperelakis, 1990; Hadley & Lederer, 1992; Fan, Yu & Palade, 2000), but only Hadley & Lederer (1992) reported effects that may be consistent with the promotion of voltage-dependent inactivation.

Our pulse protocols were specially designed to distinguish between two possible causes for the increase in voltage-dependent inactivation: a) a simple consequence of the shift in the activation curve by poising the $C \leftrightarrow O$ transition towards $O$, with no effect in other transitions, and b) a real promotion of the inactivation by favoring the occupancy of the inactivated channels, poising the equilibrium away from $O$ towards $I_o$. As the latter has been shown to be the case for antagonistic DHP (Bean, 1984; Sanguinetti and Kass, 1984) some effects of the antagonistic enantiomer R(+)Bay K were also studied to better dissect antagonistic-like effects from pure agonistic effects. Both enantiomers produced a larger negative shift on the steady-state inactivation curves than on the activation curves, which implies that both promote the occupancy of inactivated, over open-channel states, in a qualitatively similar inhibitory fashion. However, their effects differ quantitatively in: a) the agonist S(−)Bay K and not the antagonist R(+)Bay K produced a significant shift to the left in the *Q1-V* activation curve, indicating that this is a purely agonistic effect; and b) the negative shift in the inactivation curve produced by the antagonist R(+) Bay K was significantly larger than the one produced by the agonist S(−) Bay K, indicating that the former is more potent in its inhibitory properties. All the observed effects were accounted for by a modulated receptor mechanism (Hille, 1977; Bean, 1984) based on the model in Scheme 1, allowing the drugs to bind to all the states with different affinities.

## Materials and Methods

### Cell Preparation

Experiments were performed on single cardiac ventricular myocytes enzymatically isolated from guinea-pigs as previously described (Ferreira et al., 1997). Briefly, the heart was rapidly removed under deep anesthesia and mounted on a Langendorf perfusion system and perfused with normal Tyrode solution composed of (in mM) 1.8 $CaCl_2$, 145 NaCl, 5 KCl, 1 $MgCl_2$ and 10 HEPES (pH 7.3–7.4). After the coronaries were cleaned of blood, the perfusate was switched to Tyrode without Ca for about 10 min. The enzymatic solution, 1 mg/ml collagenase Type 1A and 0.2 mg/ml protease type XIV (Sigma dissolved in Tyrode 0 Ca, was then applied and recirculated for 5–8 minutes, the time depending on the degree of digestion. The enzyme solution was washed out with Tyrode 0.2 mM $CaCl_2$ and thereafter the heart was cut into pieces that were gently stirred to separate the myocytes. The whole procedure was carried out at 35–38°C. The cells were stored at room temperature in normal Tyrode solution and used within 12 hours from isolation.

### Electrophysiology and Solutions

Whole-cell recording (Hamill et al., 1981) of small rod-shaped myocytes (60–150 pF) was done with an Axopatch ID and CV4-100 headstage (Axon Instruments). Series resistance (6–8 MΩ) was partially compensated (50–70%) and capacitative transients were compensated as much as possible to avoid saturation of the amplifier. Currents were acquired at 10 kHz with an 8-bit D/A board (Tekmar TL-100) and filtered at 2 kHz. PClamp 5 software (Axon Instruments Inc.) was used for data acquisition and analysis. Controls for subtraction of non-compensated linear capacitive currents were recorded 100 ms after applying a subtracting holding potential ($V_h$) of −150 mV and were ≤20 mV in amplitude in the negative direction (i.e., to −170 mV). Four or more control pulses were averaged per test pulse. The voltage range used lies outside the nonlinear charge movement range, particularly that of Q2 based on our measurements on depolarized cells (*see* Fig. 2). The linearity of these controls was tested by subtraction from controls applied from +50 mV to +70 mV, a procedure that yielded an essentially flat difference as previously reported (Ferreira et al., 1997). The subtracting $V_h$ was applied before the sequence of conditioning and test pulses, the duty cycle for the application of the complete set of pulses was five seconds or longer to avoid accumulation of inactivation in the availability studies. The linear capacitance of the cells measured in these

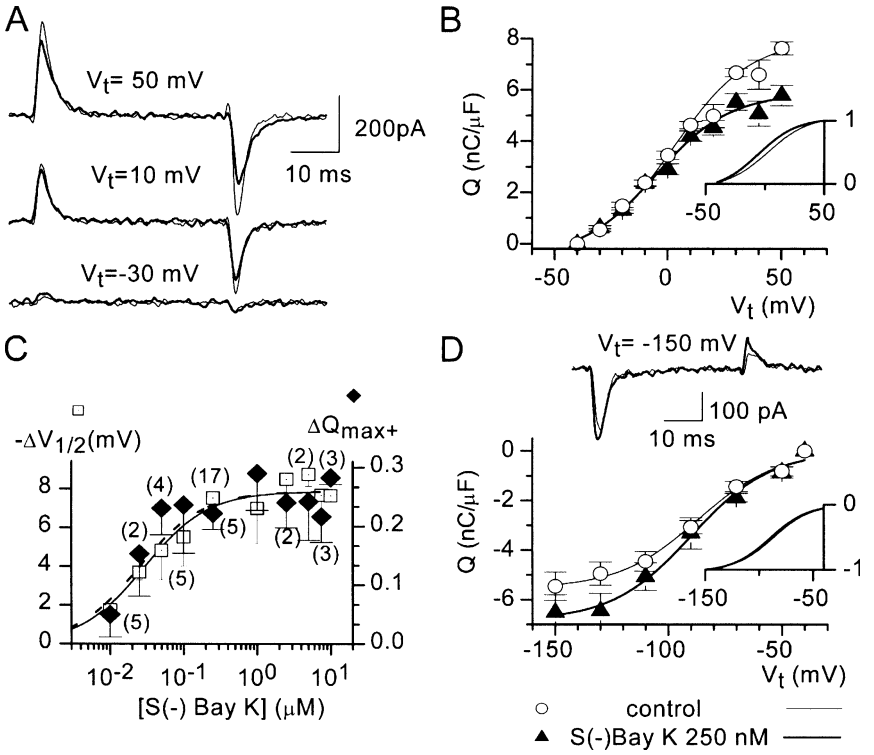


**Fig. 1.** Effect of S(−)Bay K 8644 on the *Q1* and *Q2* gating currents. (*A*) Superimposed gating currents elicited by depolarizing pulses to the indicated voltages, from $V_h = -40$ mV, in control condition (*thin traces*) and in the presence of 250 nM S(−)Bay K (*thick traces*). (*B*) *Q1 vs. V* curves plotting the charge moved during the ON transient in traces like those in *A*. Open circles are averages in absence and filled triangles in the presence of S(−)Bay K. The line plots are the fit of Eq. 1 to the mean data ($n = 17$) with parameters: $Q_{max} = 8.0$ nC/μF, $V_{1/2} = 2.2$ mV and $k = 17$ mV in control (*thin line*) and $Q_{max} = 5.9$ nC/μF, $V_{1/2} = -5.4$ mV and $k = 16$ mV in the presence of S(−)Bay K (*thick line*). These fits are also shown normalized in the inset to illustrate the difference in $V_{1/2}$ before (*thin line*) and after (*thick line*) application of S(−)Bay K. (*C*) Superimposed concentration dependence of the fraction of $Q1_{max}$ suppressed by the drug, $\Delta Q1_{max}$ ($Q1_{max}$ control−$Q1_{max}$ drug)/$Q1_{max}$ control, shown as filled diamonds (*right axis*), and the shift induced in the half-distribution potential, displayed as open squares (*left axis*). Each point represents averaged data from *n* experiments, and the vertical bars are the SEM. The lines represent the fits of single-site binding isotherms (Eq. 3) to each set of data. Best-fit parameters were: $\Delta Q1_{max} = 0.26$ (26% reduction), $K_{0.5} = 24.4$ nM (*dashed line*), and $\Delta V_{1/2max} = -7.9$ mV and $K_{0.5} = 28.8$ nM (*continuous line*). (*D*) *Top*, superimposed traces of the gating currents elicited by a hyperpolarizing pulse from $V_h = -40$ mV to −150 mV in the absence (*thin line*) and presence (*thick line*) of 250 nM S(−)Bay K. *Bottom*, charge moved during the ON transients of pulses to different test voltages. Points are means of 8 cells; circles were in control condition and triangles after application of S(−)Bay K. The line plots are the fits of Eq. 1 to each set of data, with parameters: $Q_{max} = -5.5$ nC/μF, $V_{1/2} = -87$ mV, $k = 17.5$ mV in control (*thin line*), and $Q_{max} = -6.8$ nC/μF, $V_{1/2} = -89.5$ mV, $k = 17.5$ mV in the presence of drug (*thick line*). These fits are also shown normalized in the inset with the same line code.

controls was 126 ± 5 pF in reference and 122 ± 5 pF after application of Bay K ($n = 56$). If the capacitance change exceeded 10% the cell was discarded for analysis. The remaining time-independent leak after subtraction of the controls was eliminated by subtracting a constant (obtained from a fit to the final 5 ms before the end of the pulse for the ON, or 25 ms after the end of the pulse for the OFF direction) to the corresponding segments of the records. The charge movement at ON was measured by integrating the transient current during the first 15 ms of the pulse, and that at OFF, by integrating over the first 25 ms after the pulse ended. Measurements are presented as averages ± standard error of the mean (SEM).

Pipettes (1–6 MΩ) were pulled from capillary glass #7052 (WPI, Sarasota, FL) and filled with an internal solution composed of (in mM) 100 Cs glutamic acid, 25 tetraethylammonium (TEA)Cl, 10 HEPES, 10 EGTA, 5 MgATP and 1 $MgCl_2$, pH 7.4–7.6 with CsOH. The extracellular solution contained (in mM) 80 TEACl, 50 CsCl, 3 $CdCl_2$, 0.2 $LaCl_3$, 0.03 $GaCl_3$, 1 $CaCl_2$, 1 $MgCl_2$ and 10 HEPES (pH 7.3–7.4 with TEAOH). For measurement of Ba ionic currents the trivalent blockers La and Ga were omitted, and 4 mM $BaCl_2$ substituted $CaCl_2$ and $CdCl_2$, 0.1 mM EGTA was added to chelate contaminant free Ca.

10 mM stock solutions in DMSO (dimethylsulfoxide) of the pure enantiomers of Bay K 8644, S(−)Bay K 8644 and R(+)Bay K 8644 (RBI), were stored in the dark, at 4°C. These solutions were dissolved in the external solution to the final drug concentrations. Final DMSO concentration was ≤0.1%, a concentration known to have no effects on Ca channels (Hess, Lansman & Tsien, 1984). Except for the experiments to study the dose-response curves (*see* Fig. 1*C* for the agonist and Fig. 5*C* and *D* for the antagonist), all the experiments were conducted using saturating concentrations of each drug. Measurements in the presence of Bay K 8644 were started 2 minutes after the complete exchange of the solution in the recording chamber. To completely eliminate the drugs from the tubes and chamber we replaced the latter two after

**Table 1.** Effects of S(−)- and R(+)Bay K 8644 on the parameters from Boltzmann fits to the date from individual cells

| | 250 nM S(−)Bay K 8644 | | 1 μM R(+)Bay K 8644 | |
|---|---|---|---|---|
| | Mean ± SEM | *n* | Mean ± SEM | *n* |
| Activation curves | | | | |
| $\Delta Q1_{max}$ (nC/μF) | 1.7 ± 0.2 | 17 | 2.0 ± 0.2 | 7 |
| $\Delta V_{1/2,Q1}$ (mV) | −7.52 ± 0.83 | 17 | −2.9 ± 1.1* | 14 |
| $G$ (drug/control) | 2.03 ± 0.18 | 6 | 0.7 ± 1.5 | 3 |
| $\Delta V_{1/2,G}$ (mV) | −7.7 ± 2.2 | 6 | 0.53 ± 0.04 | 3 |
| $\Delta Q2_{max}$ (nC/μF) | −1.4 ± 0.4 | 8 | −1.8 ± 0.14 | 3 |
| Availability curves | | | | |
| $\Delta Q1_{Ca}$ (nC/μF) | 1.0 ± 0.4 | 8 | 2.0 ± 0.6 | 3 |
| $\Delta V_{1/2}Q1$ (mV) | −14.8 ± 1.7 | 7 | −24.6 ± 1.2 | 3 |
| $\Delta Q2_{Ca}$ (nC/μF) | −0.85 ± 0.22 | 8 | N/A | |
| $\Delta V_{1/2}Q2$ (mV) | −18.5 ± 5.8 | 6 | N/A | |
| $\Delta V_{1/2}I_{Ba}$ (mV) | −15.2 ± 2.7 | 3 | N/A | |

*Data from 14 $Q$-$V$ curves taken with 1, 5 and 10 μM R(+)Bay K in 8 cells.

each experiment, and before reuse, the chambers were cleaned with ethanol and exposed to UV light for several (≥6) hours to completely eliminate drugs.

One Boltzmann function (equation 1), two Boltzmann functions plus a constant (equation 2), a single-site binding isotherm (equation 3) were fitted to the corresponding data by least squares routines.

$$Q(V) = Q_{max}\{1 + \exp[-(V - V_{1/2})/k]\}^{-1} \quad (1)$$

$$Q_{total} = Q_s + Q_{Na}\{1 + \exp[(V - V_{Na})/k_{Na}]\}^{-1} + Q_{Ca}\{1 + \exp[(V - V_{Ca})/k_{Ca}]\}^{-1} \quad (2)$$

$$X = X_{max}[\text{Bay K}]/(K_{0.5} + [\text{Bay K}]) \quad (3)$$

The statistical significance of the effects of drug application (negative shifts in the $Q$ *vs.* $V$ distributions and availability curves) was estimated by $t$-test (at $p \leq 0.05$) performed on the mean of the change in each parameter evaluated in each cell (to offset cell-to-cell variations). The same procedure was used to estimate the significance of the difference between the effects of the two drugs.

## Results

### S(−)Bay K 8644 Shifts the Q1-$V_{test}$ Curve to the Left

As most of the nonlinear charge that moves positive to −40 mV is due to activation-deactivation transitions of VLCC (Bean & Ríos, 1989; *see* also Fig. 3, below) we first used this holding potential ($V_h$) to study the effects of 250 nM S(−)Bay K on the gating currents and charge distribution with test pulses to different voltages (Fig. 1). The current traces obtained in response to pulses to +50 mV in the absence (thin line) and presence of drug (thick line) are superimposed. The charge moved in the ON direction of the pulse equaled that moved in the OFF direction if the test pulses were shorter than 20 ms. For 20-ms long pulses, in the control condition the ratio between the charge moved during the ON and that moved during the OFF transient ($Q_{ON}/Q_{OFF}$) was 1.09 ± 0.03. In the presence of 250 nM S(−)Bay K this ratio was increased to 1.23 ± 0.07, the mean increment in this ratio was 13 ± 5% ($n$ = 12). In the presence of S(−)Bay K 8644 the time course of the OFF transient after depolarizing test pulses was slowed down compared to the control condition. Its decay, after test pulses to +50 mV, was well described by a single exponential with time constants, $\tau_{OFF}$, 1.6 ± 0.1 ms, and 2.5 ± 0.2 ms, in absence, and in the presence of 250 nM S(−)Bay K 8644, respectively. The mean increase in the time constant was 60 ± 7% ($n$ = 17).

Fig. 1*B* shows the charge moved during the ON transient as a function of the test voltage for depolarizing pulses, the $Q1$ *vs.* $V$ distribution. The parameters obtained from the fit of a single Boltzmann function (Eq. 1, Methods) to the data from individual cells yielded the parameters given in Table 1. Compared to the control condition (*open circles*), the presence of drug (*filled triangles*) induced a reduction of 1.7 ± 0.2 nC/μF ($n$ = 17) in $Q1_{max}$ (the maximum charge moved with activating pulses), and a negative shift $\Delta V_{1/2}$ = −7.5 ± 0.8 in the half distribution voltage ($n$ = 17). The curves fitted to the mean data in the presence (*thick line*) and absence (*thin line*) of S(−)Bay K 8644 are also shown normalized in the inset, to illustrate the shift in $V_{1/2}$. All these observations were consistent with previous reports using similar pulse protocols (Hadley and Lederer, 1992; Fan et al., 2000).

The concentration dependence (Fig. 1*C*) for the effects on $\Delta V_{1/2}$ (*open squares*) and $Q1_{max}$ (*filled diamonds*) were very similar. The fit of single-site binding isotherms gave $K_{0.5}$ ~25 nM in both cases. Therefore we used 250 nM S(−)Bay K as a saturating concentration to study all the effects of the drug.

A different set of experiments was carried out to explore the effects of the drug on the charge move-

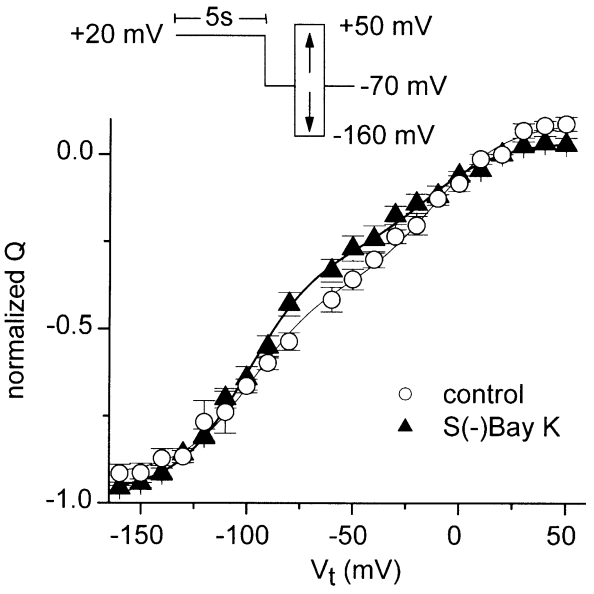


**Fig. 2.** Effect of S(−)Bay K on the charge movement distribution in maximally inactivated cells. Charge distribution after maximal inactivation was achieved by a 5-s long conditioning pulse to +20 mV, measured in the ON transients of test pulses to various potentials (protocol illustrated in the inset). Two Boltzmann components (Eq. 2) were necessary to describe the average data from 6 cells. Best-fit parameters were: $Q1 = 0.463$, $Q2 = 0.549$, $V_1 = -12.0$ mV, $V_2 = -96.8$ mV and in Bay K $Q1 = 0.31$, $Q2 = 0.69$, $V_1 = -14.7$ mV, $V_2 = -99.2$ mV. In both curves the slope factors were set to the same value, $k_1 = k_2 = -17$ mV. The data were normalized to the total charge of each cell (mean 12.69 ± 0.96 nC/μF) to highlight the small differences between the two curves and the 0 charge was set at the conditioning voltage.

ment negative to $V_h = -40$ mV (Fig. 1*D*), presumably reflecting mostly *Q2* originated in Ca as well as Na channels. The traces obtained with pulses to −150 mV in the absence (*thin line*) and presence (*thick line*) of 250 mM S(−)Bay K illustrate the increase in the maximum charge moved in this range of voltage. The "*Q2*" *vs. V* distributions for hyperpolarizing pulses in the absence (*open circles*) and presence (*filled triangles*) of drug are shown in Fig. 1*D*, bottom. The fits of single Boltzmann distributions to the *Q2 vs. V* curves in individual cells yielded an average increase of 1.4 ± 0.4 nC/μF ($n = 8$) in the maximum movable charge. This increase in $Q2_{max}$ is not significantly different from the just described reduction in $Q1_{max}$. The midpoint of the distribution is not significantly modified, as illustrated in the inset, which shows the normalized best fit of Boltzmann functions to the mean data.

The negative shift in $V_{1/2}$ of the *Q1 vs. V* curve indicates the stabilization of the open channel state(s) with respect to the closed ones. The reciprocal changes in $Q1_{max}$ and $Q2_{max}$ might be an indication of an increased voltage-dependent inactivation, an interpretation further supported by the data presented below.

## S(−)Bay K 8644 Does not Shift the Distribution between Inactivated States

Due to the partial superposition of the *Q1* and *Q2* distributions and the smaller size of the latter at $V_h = -40$ mV, this condition is inappropriate to accurately measure the $V_{1/2}$ of *Q2*. This is an important parameter as it contributes to set the mid voltage of the availability curve (*see* Eq. A2 in the Appendix). The best conditions for this measurement are obtained after holding the membrane at depolarized potentials (>0 mV) in order to achieve maximal inactivation (Shirokov et al., 1992). Fig. 2 shows data from 6 cells in which we measured the charge moved during the ON transition of test pulses to different test voltages after a conditioning pulse of 5 seconds to 20 mV and a 30-ms long interpulse to −70 mV (as schematized in the inset). The total charge measured in this condition was 13 ± 1 nC/μF, the same as under other conditions (e.g., Figs. 1 and 3).

Consistent with an incomplete voltage-dependent inactivation previously reported for ionic currents (Hadley & Hume, 1987) and gating currents (Bean & Ríos, 1989), at least the sum of two Boltzmann distributions were necessary to describe the data. The $V_{1/2}$ corresponding to *Q2* (including charge from Ca- as well as Na-channels) was not modified by 250 nM S(−)Bay K. As the shift in *Q1 vs. V* is an indication of higher affinity for activated (open) than for the closed channels, the absence of a significant shift in the *Q2 vs. V* distribution indicates that the drug does not favor any particular state among inactivated states of the channel (*see* Appendix). The reduction in *Q1* induced by the drug (which in all likelihood is only due to Ca channels) from 0.45 to 0.31 reflects an increase in the maximum level of inactivation, consistent with higher affinity for inactivated states.

## S(−)Bay K Shifts the Availability Curves of *Q1* and *Q2*

The reductions in $Q1_{max}$ described in Figs. 1 and 2 are consistent with promotion of voltage-dependent inactivation by the agonistic enantiomer. Next, we studied the effect of 250 nM S(−)Bay K on the voltage dependence of steady-state inactivation, measuring the availability curves (Fig. 3) for *Q1* (Fig. 3*A*) and *Q2* (Fig. 3*B*). The pulse protocols[1] used are schematized in the figure and consisted in 5 s at the corresponding conditioning voltages ($V_c$), a 30-ms interpulse to −70 mV, and finally the test pulse, to

[1]This protocol (also used by Shirokov et al., 1992) simplifies the separation between *Q1* and *Q2*, as it allows non-inactivated channels to return to the resting closed state during the interpulse at −70 mV and it allows the dissection of the charge moved by VLCC ($Q_{Ca}$) from that moved by Na channels ($Q_{Na}$).

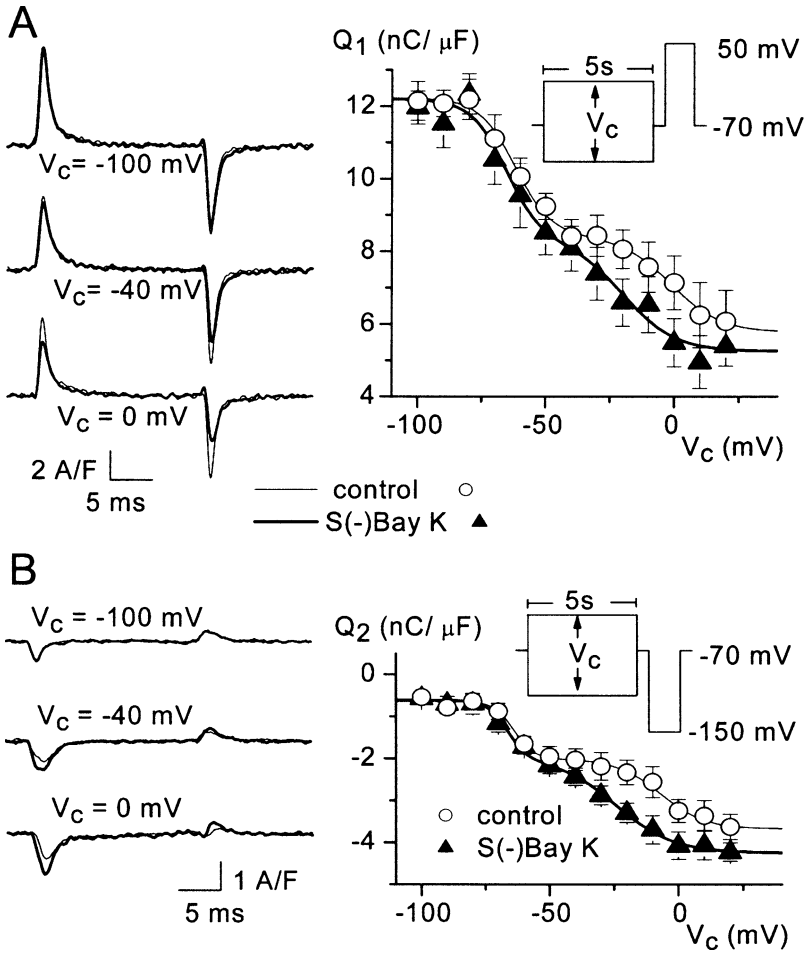


**Fig. 3.** Effect of S(-)Bay K on steady-state availability curves. (*A*) *Q1* availability measured with the pulse protocol schematized in the inset and described in the text. *Left*, gating current records from one cell. Thin traces correspond to control conditions and thick traces were in the presence of 250 nM S(−)Bay K. *Right*, ON charge plotted against conditioning voltage ($V_c$) summarizing data from 8 cells. Circles are control, and triangles in the presence of drug. The fits of two Boltzmann functions plus a constant (Eq. 2) are shown as a thin line for control and a thick line for S(−)Bay K. The best-fit parameters were: $Q_s$ = 5.8 nC/μF; $Q_{Na}$ = 3.8 nC/μF, $V_{Na}$ = −62 mV, $k_{Na}$ = 7.0 mV, $Q_{Ca}$ = 2.7 nC/μF, $V_{Ca}$ = −1.3 mV and $k_{Ca}$ = 9.6 mV, for the control condition, and $Q_s$ = 5.3 nC/μF, $Q_{Na}$ = 3.9 nC/μF, $V_{Na}$ = −65 mV, $k_{Na}$ = 6.9 mV, $Q_{Ca}$ = 3.1 nC/μF, $V_{Ca}$ = −19.5 mV and $k_{Ca}$ = 10 mV, in the presence of drug. (*B*) *Q2* availability measured with the pulse protocol schematized in the inset. *Left*, gating current records with same trace code as in *A*. On the right, points are mean ($n$ = 11) ON charge in the test pulse to −150 mV plotted against conditioning voltage; same symbol code as in *A*. Lines are the fits of Eq. 2 to each set of data; same line code as *A*. Best fit parameters were: $Q_s$ = −0.5 nC/μF; $Q_{Na}$ = −1.4 nC/μF, $V_{Na}$ = −64 mV, $k_{Na}$ = −3.9 mV, $Q_{Ca}$ = −1.7 nC/μF, $V_{Ca}$ = −6.9 mV and $k_{Ca}$ = −8.6 mV, for the control condition, and $Q_s$ = −0.6 nC/μF, $Q_{Na}$ = −1.4 nC/μF, $V_{Na}$ = −65.5 mV, $k_{Na}$ = −3.9 mV, $Q_{Ca}$ = −2.3 nC/μF, $V_{Ca}$ = −24 mV and $k_{Ca}$ = −11 mV after application of S(−)Bay K.

+50 mV to measure *Q1*, or to −150 mV to measure *Q2*. The left hand panels of Fig. 3*A* (*Q1*) and Fig. 3*B* (*Q2*) display the gating current records after conditioning pulses to the indicated voltages, in the absence (*thin traces*) and presence (*thick traces*) of 250 nM S(−)Bay K. The points in the graph of the right-hand panels represent the mean data from different groups of cells used to study *Q1* and *Q2* availability. Circles are in control and triangles in the presence of 250 nM S(−)Bay K.

Despite the slight difference (non-significant according to a *t*-test, *see* Table 1) in the total charge measured in the curve for *Q2*, it is clear that it is measuring the same phenomenon than the curve for *Q1*. The two availability curves were fitted (line plots) with the sum of two Boltzmann functions plus a constant (Eq. 2) in the absence (*thin line*) and presence of drug (*thick line*). The two Boltzmann components are readily identifiable as due to inactivation of Na channels, centered at ∼ −65 mV, and to inactivation of Ca channels, the center of which is clearly shifted and its amplitude slightly increased by S(−)Bay K. An important fact is that only the Ca-channel component was affected, consistent with the specificity of DHPs action. Table 1 gives the mean change produced by S(−)Bay K in the parameters obtained by fitting to the data from individual cells. In particular, the voltages of half inactivation were −14.8 ± 1.7 mV ($n$ = 7) for *Q1*, and −18.5 ± 5.8 mV ($n$ = 6) for *Q2*. Both roughly double and are significantly larger (at $p$ = 0.01, both for *Q1* and *Q2*) than the −7.5 mV shift observed in the *Q1 vs. V* previously described.

### Effect of S(−)Bay K on $I_{Ba}$ Activation and Inactivation

Given the data described above it was important to establish how the observed effects on gating currents are correlated with the effect of S(−)Bay K 8644 on ionic current through VLCC, a more faithful indication of the occupation of the open state(s). Ba currents (Ba was used to diminish current-dependent effects) were measured at different test voltages from $V_h$ = −50 mV (Fig. 4*A*) in the absence (*thin trace*) and then in the presence of 250 nM S(−)Bay K (*thick trace*). The data from $I_{peak}$-$V$ curves (*not shown*) was analyzed to construct the conductance *vs.* voltage ($G_{Ba}$-$V$) curve, shown normalized to the conductance at +20 mV in the control condition in Fig. 4*B*. The

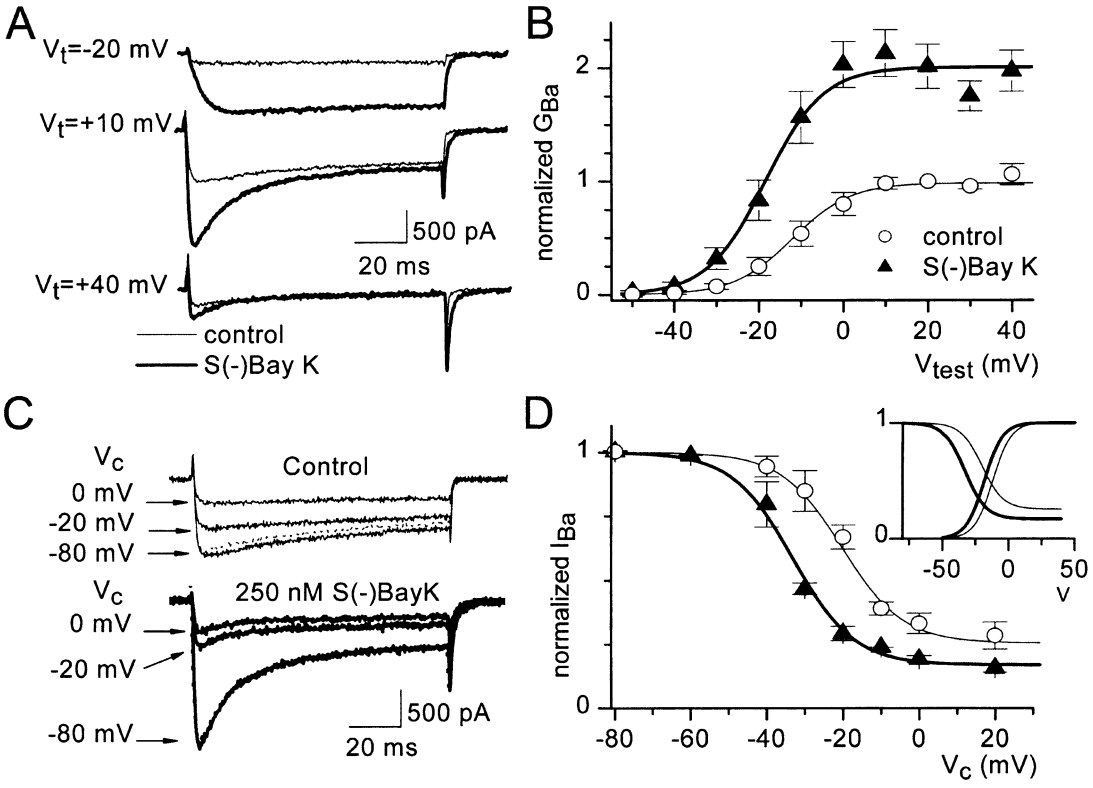


**Fig. 4.** Effect of S(−)Bay K on $Ba^{2+}$ currents. (*A*) Ionic currents carried by 4 mM Ba, elicited by depolarizing test pulses to the indicated voltages $V_t$, from $V_h = -50$ mV, both in the control condition (*thin traces*) and in presence of 250 nM S(−)Bay K (*thick traces*). (*B*) Normalized $G_{Ba}$ *vs.* *V* curves obtained from records like those in Fig. 1*A*, as explained in the text. Circles are averages ($n = 6$) in control and triangles in S(−)Bay K. The line plots are the fits of a single Boltzmann distribution (*A* substituting $Q_{max}$ in Eq. 1) with parameters $A = 1$, $V_{1/2} = -12.1$ mV, $k = 7$ mV in control (*thin line*) and $A = 2$, $V_{1/2} = -18.4$ mV, $k = 7$ mV in the presence of S(−)Bay K. (*C*) $I_{Ba}$ was measured with identical conditioning and interpulse as in Fig. 3, using a test pulse to +10 mV. *Top*, current records in control conditions after a conditioning pulse to the voltages indicated at the left. The dashed line trace ($V_c = -80$ mV) was obtained after the pulses to −20 and 0 mV to quantify the rundown. *Bottom*, records in the presence of 250 nM S(−)Bay K; the dashed line trace is not evident due to complete absence of rundown in this cell in this condition; all the traces in *A* and *C* were from the same cell. (*D*) Data summarizing the inactivation curves obtained in 3 cells normalized to the current measured after $V_c = -80$ mV. Open circles are control, and filled triangles in 250 nM S(−)Bay K. The fits of a Boltzmann function plus a constant gave parameters: $A = 0.75$, $V_{1/2} = -20.2$ mV, $k = 8$ mV, $A_s = 0.25$ for control (*thin line*), and $A = 0.83$, $V_{1/2} = -33$ mV, $k = 8$ mV, $A_s = 0.17$ in the presence (*thick line*) of S(−)Bay K. All the curves fitted in *D* and *B*, are shown together, normalized, in the inset, illustrating the difference in $\Delta V_{1/2}$ for activation and inactivation curves.

mean data from 6 cells clearly shows that the maximal conductance is doubled after application of the drug (*triangles*) compared to the control condition (*circles*). But the drug also induced a shift of $-7.7 \pm 2.2$ mV ($n = 6$) in the half-distribution voltage of the fits of a Boltzmann function (Eq. 1) to the data from individual cells (Table 1 also summarizes the effects in Ba currents). Fig. 4*C* displays the Ba currents measured after 5-s conditioning pulses to the indicated voltages in the absence (*top*) and presence of 250 nM S(−)Bay K (*bottom*). The pulse protocol was identical to those in Fig. 3*A*, except for the test pulse, which was to +10 mV. After the measurements with conditioning pulses to −20 and 0 mV we repeated the measurement with a conditioning voltage to −80 mV (*dotted line*) to monitor the rundown. Figure 4*D* displays the mean data from 3 cells (normalized to $I_{Ba}$ for $V_C = -80$ mV in each cell under each condition) in which we measured the availability in the absence (*circles*) and presence (*triangles*) of S(−)Bay K. The fit of a single Boltzmann distribution yielded the parameters included in Table 1. In particular, the drug induced a shift of $-15.2 \pm 2.7$ mV in $V_{1/2}$ and an increase of the maximal $I_{Ba}$ inactivation. Thus, the ionic current data reassert those obtained with charge movement: the shift induced by the drug on the $G_{Ba}$ *vs.* *V* curve is of smaller amplitude than the shift produced in the availability curve. Furthermore, the actual values of the shifts induced in $I_{Ba}$ activation and inactivation were very similar to those induced in the activation and inactivation curves for *Q1*.

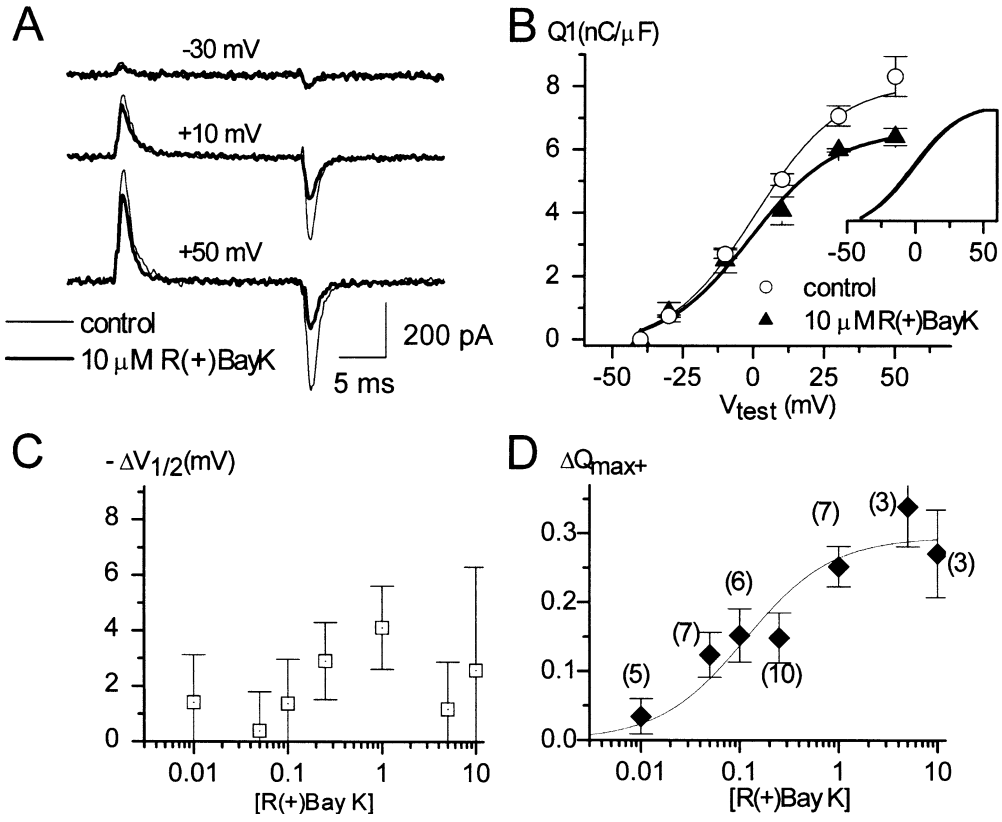


**Fig. 5.** Effects of R(+)Bay K 8644 on *Q1-V* distribution. (*A*) Gating currents elicited by depolarizing pulses to the indicated voltages, from $V_h = -40$ mV, both in control (*thin traces*) and in the presence of 10 μM R(+)Bay K (*thick traces*). (*B*) ON charge before (*circles*) and after (*triangles*) application of 10 μM R(+)Bay K ($n = 3$). The line plots represent the fit of Eq. 1 to the data with parameters $Q1_{max} = 8.1$ nC/μF, $V_{1/2} = 0.6$ mV, $k = 15$ mV, previous to application of drug and $Q1_{max} = 6.6$ nC/μF, $V_{1/2} = -1.3$ mV, $k = 15$ mV in the presence of R(+)Bay K. These fits are also shown normalized in the inset with the same line code. (*C*) Concentration dependence for the effect in $\Delta V_{1/2}$. Note the large variability (for each concentration $n$ is shown in *D*) and smaller amplitude of the shift, which does not clearly increase with [R(+)Bay K]. (*D*) Concentration dependence of the fractional reduction in $Q1_{max}$. Diamonds are averages in $n$ experiments. The line plot represents the best fit of Eq. 3 to the data, with parameters: $\Delta Q1_{max} = 32\%$ and $K_{0.5} = 150$ nM.

## R(+)Bay K 8644 only Promotes Inactivation

The two enantiomers of Bay K 8644 have opposite effects in the $P_o$ of VLCC (Kass, 1987; Hering et al., 1993). Because at the gating-current level the agonist behaved mainly as would have been expected for an antagonist, mostly promoting voltage-dependent inactivation, we explored the effects of the antagonist enantiomer, R(+)Bay K 8644 (Figs. 5 and 6) in an attempt to better dissect agonistic from antagonistic effects. Figure 5*A* displays the gating currents measured with test pulses to the indicated voltages from $V_h = -40$ mV in the absence (*thin line*) or presence of 10 μM R(+)Bay K 8644 (*thick line*). Consistent with an increased voltage-dependent inactivation, the antagonistic enantiomer reduced $Q1_{max}$. The drug also induced a larger $Q_{ON}/Q_{OFF}$ ratio than the agonist. This quantity changed from 1.08 ± 0.02 in reference to 1.51 ± 0.17 in R(+)Bay K ($n = 9$), indicating a larger voltage-dependent inactivation during the 20 ms pulse. At variant with the S(−) enantiomer the time course of the OFF transient upon repolarization was not significantly modified. The points in Fig. 5*B* represent the mean data from 3 cells in which we studied the effect of 10 μM R(+)BayK on the *Q1 vs. V* distribution. The average changes induced by the drug in the parameters obtained by fits of single Boltzmann functions to the data of individual cells is reported in Table 1. 1 μM R(+)Bay K reduced $Q1_{max}$ by 24 ± 3%. The shift in the $V_{1/2}$ of the *Q1* distribution was −2.9 ± 1.1 mV ($n = 8$), significantly smaller than the one produced by the agonist. It also did not have a clear dependency on [R(+)Bay K] (Fig. 5*C*). On the other hand, the dose-response curve for the reduction in $Q1_{max}$ (Fig. 5*D*) was well fitted with a one-to-one binding isotherm with parameters $\Delta Q1_{max} = 32\%$, and $K_{0.5} = 150$ nM. The lower apparent affinity found for the antagonist enantiomer than for the agonist is consistent with previous studies (Hamil-

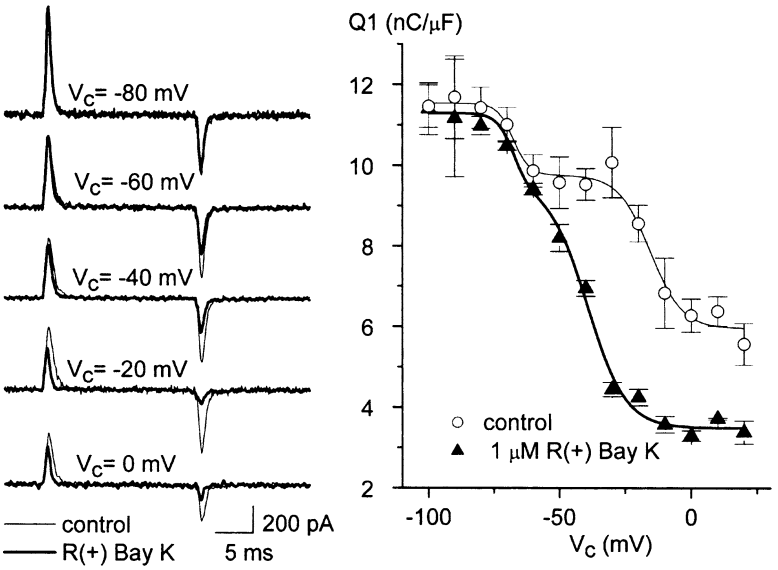


**Fig. 6.** Effect of R(+)Bay K on the steady-state availability curve for *Q1*. The availability of *Q1* was measured as in the experiments of Fig. 3*A*, above. *Left*, superimposed gating current records obtained after conditioning pulses to the indicated $V_c$ in control (*thin traces*) and in the presence of 1 μM R(+)Bay K (*thick traces*). Right, average data from 3 cells in which *Q1*-$V_c$ curves were studied in the absence (*circles*) and then in the presence (*triangles*) of 1 μM R(+)Bay K. The line plots represent the fit of Eq. 2 to the data with parameters $Q_{Ca}$ = 4.0 nC/μF, $V_{Ca}$ = −14 mV, $k_{Ca}$ = 9 mV, $Q_{Na}$ = 1.7 nC/μF, $V_{Na}$ = −68, $k_{Na}$ = 2.4 mV, $Q_s$ = 6.0 nC/μF in the control condition (*thin line*), and $Q_{Ca}$ = 6.0 nC/μF, $V_{Ca}$ = −39.3 mV, $k_{Ca}$ = 7.2 mV, $Q_s$ = 3.5 nC/μF in the presence of drug (*thick line*).

ton et al., 1987; Bechem, Hebisch & Schramm, 1988; Wei, Rutledge & Triggle, 1989) and justifies the use of a saturating [R(+)Bay K] ≥1 μM for the comparison with lower but also saturating concentrations of S(−)Bay K. The effects on ionic currents at $V_h$ = −40 mV of the R(+) enantiomer were also studied. While the conductance was reduced 30%, $V_{1/2}$ was not significantly changed (*see* Table 1).

Figure 6 displays the effect of R(+)Bay K on the availability curve for *Q1* measured in 3 cells. As in the case of the S(−) enantiomer, only the VLCC component was affected by the drug, being shifted to the left and increased in amplitude. However, in this case the shift was −24.6 ± 1.2 mV (*see* Table 1), significantly larger than the shift produced by S(−)Bay K in the same component ($p$ = 0.01). Based on this finding we conclude that R(+)Bay K has stronger antagonistic properties than S(−)Bay K 8644 and lacks its agonistic properties.

## Discussion

This work presents a complete study of the effect of S(−)Bay K 8644 on the gating currents of cardiac VLCC and its comparison with the effects of the antagonist R(+)Bay K 8644. Our results demonstrate that: 1) S(−)Bay K 8644 facilitates voltage-dependent inactivation as well as voltage-dependent activation and that the increase in inactivation is a direct effect, not explained by its link to activation; 2) the antagonist has almost exclusively antagonistic properties; 3) such effects are readily explained by a modulated-receptor model. In what follows these items will be discussed separately.

### Duality of S(−)Bay K 8644 Effects on VLCC Gating Currents

From the comparison between the effect of both enantiomers, we conclude that the shift to more negative potentials in the *Q1 vs. V* curve, and the slower OFF transient after depolarizing pulses previously reported by Hadley and Lederer (1992) and Fan et al. (2000), represent pure agonistic effects of S(−)Bay K 8644, because they are not produced by the R(+) enantiomer, which we show behaves as a pure voltage-dependent inhibitor of gating currents. In this respect, our data confirm and expand conclusions from previous reports on VLCC regarding whether S(−)Bay K 8644 reduces the maximum *Q1* moved by depolarizing test pulses from −50 mV. Josephson and Sperelakis (1990) and Fan et al. (2000) reported no reduction in this parameter, while Hadley and Lederer (1992) showed a reduction of 22%. The latter authors also showed larger reductions from $V_h$ = −40 and −30 mV than from −50 mV, suggesting voltage-dependent inactivation, but their results did not discard other explanations; for instance, an apparent reduction in the maximal *Q1* simply due to the shift in the activation curve making a relatively depolarized $V_h$ (i.e., −40 mV) fall within the voltage range in which *Q1* moves. In our study of the availability of *Q1* we did not observe a reduction in the maximum at $V_h \leq -50$ mV (*not shown*, but *see* availability of *Q1* at −50 mV in Fig. 3), but we did see it when $V_h \geq -40$ mV (Fig. 1). Thus, the discrepancies between previous studies could be explained by differences in $V_h$ or small shifts in the actual membrane potentials due to the use of different solutions.

The negative shift of the *Q1* distribution was consistent with the shift in $G_{Ba}$ *vs. V* curve that we found, yielding a negative shift in the mid voltage of a

Boltzmann function (Eq. 1) of almost −8 mV. As the maximum $G_{Ba}$ was increased by a factor of two while maximum *Q1* was slightly reduced, the notion that the agonistic effect should consist in more than what is observed at the gating-current level is strengthened.

As the amount of charge reduced in the *Q1 vs. V* curves is consistent with the effect on availability curves for *Q1* and *Q2* at those particular voltages, the reduction can be considered an "antagonistic" effect (i.e., promotion of inactivation). Moreover, the agonist produces a larger negative shift in the availability curves of *Q1* and *Q2* (Fig. 3) than in the *Q1 vs. V* distribution (Fig. 1). A similar difference was also observed when $G_{Ba}$ *vs. V* and $I_{Ba}$ availability were compared. Thus an unavoidable conclusion is that the inactivated states must be energetically favored by drug binding. Therefore, the inactivated states were concluded to have a higher affinity for the agonist enantiomer than the available states. Because agonistic ($\Delta V_{1/2}$) and antagonistic effects ($\Delta Q1_{max}$) are produced with remarkably similar apparent affinities (Fig. 2), the affinity of these two states should not be drastically different.

## Quantitative Distinction of the Effects of S(−) and R(+)Bay K 8644

Although both enantiomers produce qualitatively similar effects, i.e., shifting the availability curve of Ca channel gating currents to the left and increasing the amount of channels inactivated at depolarized voltages, our results show that their antagonistic effects are quantitatively distinct. When applied at saturating concentrations R(+)Bay K 8644 is more potent in promoting inactivation (therefore, as an antagonist), because the left-shift in the availability of *Q1* is significantly bigger than that induced by S(−)Bay K. Despite this stronger effect it occurs with lower affinity for the channel with a $K_{0.5}$ roughly one order of magnitude higher than S(−)Bay K 8644. This difference in affinities between the two enantiomers, consistent with previous functional (Hamilton et al., 1987; Bechem et al., 1988) and binding (Wei et al., 1989) studies, is the reason of racemic Bay K 8644 being an agonist.

## Comparison with Previous Work on Voltage-dependent Effects of Agonist DHPs on Ba Currents

At least two reports explained the antagonist effect of agonistic DHPs by two completely different mechanisms. Kamp et al. (1989) proposed that the +202-791 effect was due to an increase in voltage-dependent inactivation, while Markwardt and Nilius (1988) proposed a current-dependent model for promotion of inactivation by racemic Bay K 8644. None of these reports, however, studied the extremely positive voltage range necessary to distinguish between current- and voltage-dependent inactivation mechanisms. Our results demonstrate promotion of voltage-dependent inactivation by Bay K but do not discard effects on current-dependent processes.

It must be noted that promotion of inactivation by S(−)Bay K 8644 has, in general, not been observed in Ba currents through VLCC expressed in *Xenopus* oocytes (Lory et al., 1990; Grabner et al., 1996; Nocetti et al., 1998). This intriguing difference could be due to different subunit composition, different lipids, different degrees of phosphorylation, etc., in that preparation and somehow justifies the study of mechanistic aspects of gating in native channels.

## A Modulated Receptor Model Accounts for the Steady-state Data

In keeping with the tradition of analyzing DHP effects in the context of the modulated-receptor hypothesis (Hille, 1977), we used the modulated-receptor version (scheme II) of the four-states-model for the voltage dependence of DHP receptors (Brum & Rios, 1987; Shirokov et al., 1992) presented in the introduction, to simulate all our steady-state results. In this model, only horizontal transitions move charge. *Q1* is moved in transitions between the upper, non-inactivated, states, while *Q2* is moved between the lower, inactivated states.[2] With the parameters estimated by measuring the voltage-dependent transitions of the cycles in the absence and in the presence of saturating concentrations of DHP, it is possible to reproduce the main characteristics in all the curves. That was done for the agonist (Fig. 7) and for the antagonist (*not shown*, but *see* Appendix). In fact, what we obtained from our voltage-dependent measurements was the ratio between the affinities of the states for the drug, because the values of the constants must satisfy microscopic reversibility. The affinity of only one state is a relatively free parameter, but its possible values are constrained by the dose-response curves in Fig. 1. The actual value chosen was 20 nM, which is consistent with our data and with data from the literature (Lacerda & Brown, 1989).

The current formulation naturally explains the larger leftward shift produced by S(−)Bay K on the

[2]In the model, *Q1* and *Q2* should vary by the same amount; the availability data presented in Fig. 3 is not conclusive in this regard. The observed difference could be explained by the variability of the steady-state level of inactivation in the absence of drug (note large error bars in the availability curve for $Q1_{Ca}$ at saturating voltages) and because the measurements were done in different *groups of* cells. In any case, our qualitative conclusions about DHP's actions are not affected by this variability because we always compared the situations in the absence and in the presence of drug in the same cell. Furthermore, we found the parallel shift in mid-voltage of both availability curves to strongly support the interconversion of the *Q1* into the *Q2* mechanism.

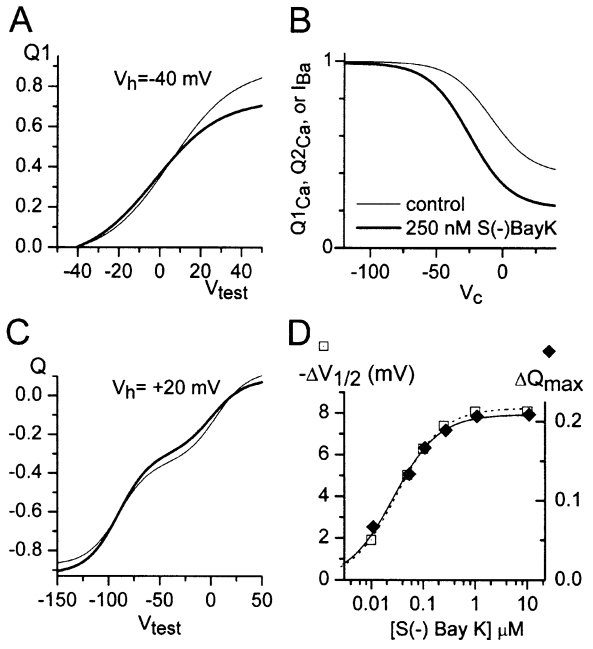


**Fig. 7.** Simulations of the steady-state curves. The model of Scheme 2 (Appendix) was used with the parameters given in the appendix to simulate the curves in the absence and presence of S(−)Bay K. (*A*) *Q1-V* curve above −40 mV in the presence (*thick line*) and absence (*thin line*) of 250 nM S(−)Bay K. (*B*) steady state availability curve of *Q1*, same line code. (*C*) Total charge distribution from a holding potential of +20 mV. (*D*) Dose-response curves obtained by simulating the *Q1-V* curves from $V_h$ = −40 mV at different concentrations of S(−)Bay K. Eq. 3 was fitted to the simulated reduction in $Q1_{max}$ (*diamonds*, *solid line*) and $-\Delta V_{1/2}$ (*squares*, *dashed line*).

availability curve than on the activation curve. This last data is impossible to reconcile with a mechanism in which the increase in inactivation is only a consequence of the shift in the activation curve. The classical form of this mechanism is embodied in the three-states sequential model proposed by Sanguinetti, Krafte and Kass (1986), in which the agonist produces a reduction in the closing rate of the drug-bound channels while the inactivation rate constants remain unchanged. As their simulations showed, such a model shifts the availability curve by the same amount as the activation curve. This would constitute what can be named "pure agonist" effect and imply the same affinity for open than for inactivated channels, as discussed in the Appendix. Thus, our data are best understood if binding with higher affinity to inactivated states by the S(−) enantiomer is accepted.

Finally, our modulated-receptor formulation also accounts for the effects of the antagonist and allows for the quantitative distinction of the antagonistic effect of S(−) and R(+) enantiomers. Considering the particular case of equal affinity for the inactivated states, a "pure agonist" would bind preferentially to the open state (and to both inactivated states), thus the shift in the availability curve would be only at the expense of the shift in the *Q1* distribution. A "pure antagonist" would bind with high affinity to the inactivated states and with equal but lower affinity to available states. The shift would result as consequence of the higher inactivation constant of the drug-bound states. This is embodied in Eq. A3 of the Appendix, which shows that the relative contribution of these "pure" effects and the overall shift itself depend on the ratios rather than on the actual values of the dissociation constants.

## References


Bean, B.P. 1984. Nitrendipine block of cardiac calcium channels: high-affinity binding to the inactivated state. *Proc. Natl. Acad. Sci.* USA **81:**6388–6392

Bean, B.P., Ríos, E. 1989. Nonlinear charge movement in mammalian cardiac ventricular cells. Components from Na and Ca channel gating. *J. Gen. Physiol.* **94:**65–93

Bechem, M., Hebisch, S., Schramm, M. 1988. $Ca^{2+}$ agonists: new sensitive probes for $Ca^{2+}$ channels. *Trends Pharmacol. Sci.* **9:**257–261

Bezanilla, F., Taylor, R.E., Fernandez, J.M. 1982. Distribution and kinetics of membrane dielectric polarization. I. Long-term inactivation of gating currents. *J. Gen. Physiol.* **79:**21–40

Brum, G., Ríos, E. 1987. Intramembrane charge movement in skeletal muscle fibers. Properties of charge 2. *J. Physiol.* **387:**489–517

Brum, G., Fitts, R., Pizarro, G., Ríos, E. 1988. Voltage sensors of the frog skeletal muscle membrane require calcium to function in excitation-contraction coupling. *J. Physiol.* **398:**475–505

Fan, J.S., Yu, Y., Palade, P. 2000. Kinetic effects of FPL 64176 on L-type $Ca^{2+}$ channels in cardiac myocytes. *Naunyn Schmiedebergs Arch. Pharmacol.* **361:**465–476

Ferreira, G., Artigas, P., Pizarro, G., Brum, G. 1997. Butanedione monoxime promotes voltage-dependent inactivation of Ca channels in heart: Effects on gating currents. *J. Mol. Cell. Cardiol.* **29:**777–787

Grabner, M., Wang, Z., Hering, S., Striessnig, J., Glossman, H. 1996. Transfer of 1,4-dihydropyridine sensitivity from L-type to class A (BI) calcium channels. *Neuron.* **16:**207–218

Hadley, R., Lederer, R.W. 1992. Comparison of the effects of Bay K 8644 on cardiac $Ca^{2+}$ currents and $Ca^{2+}$ channel gating current. *Am. J. Physiol.* **262:**H472–H477

Hadley, R.W., Hume, J.R. 1987. An intrinsic potential-dependent inactivation mechanism associated with calcium channels in guinea-pig myocytes. *J. Physiol.* **389:**205–222

Hamilton, S.L., Yatani, A., Brusch, K., Schwartz, A., Brown, A.M. 1987. A comparison between the binding and electrophysiological effects of dihydropyridines on cardiac membranes. *Mol. Pharmacol.* **31:**221–231

Hamill, O.P., Marty, A., Neher, E., Sakmann, B. 1981. Improved patch-clamp techniques for high resolution current recording from cells and cell free membrane patches. *Pfluegers. Arch.* **391:**85–100

Hering, S., Hughes, A.D., Timin, E.N., Bolton, T.B. 1993. Modulation of calcium channels in arterial smooth muscle cells by dihydropyridine enantiomers. *J. Gen. Physiol.* **101:**393–410

Hess, P., Lansman, J., Tsien, R.W. 1984. Different modes of $Ca^{2+}$ channel gating behavior favored by dihydropyridine Ca agonist and antagonist. *Nature* **311:**536–544

Hille, B. 1977. Local anesthetics: hydrophilic and hydrophobic pathways for the drug-receptor reaction. *J. Gen. Physiol.* **69:** 497–515

Josephson, I.R., Sperelakis, N. 1990. Fast activation of cardiac $Ca^{2+}$ channel gating charge by the dihydropyridine agonist BayK 8644. *Biophys. J.* **58:**1307–1311

Kamp, T., Sanguinetti, M.C., Miller, R.J. 1989. Voltage- and use-dependent modulation of cardiac calcium channels by dihydropyridine (+) 202–791. *Circ. Research.* **69:**338–351

Kass, R.S. 1987. Voltage-dependent modulation of cardiac calcium channel current by optical isomers of Bay K 8644: Implications for channel gating. *Circ. Research* **61:**11–15

Lacerda, A.E., Brown, A.M. 1989. Non-modal gating of cardiac calcium channels as revealed by dihydropyridines. *J. Gen. Physiol.* **93:**1243–1273

Lory, P., Rassendren, F.A., Richard, S., Tiaho, F., Nargeot, J. 1990. Characterization of voltage-dependent calcium channels expressed in *Xenopus* oocytes injected with mRNA from rat heart. *J. Physiol.* **429:**95–112

Markwardt, F., Nilius, B. 1988. Modulation of calcium channel currents in guinea-pig single ventricular heart cells by the dihydropyridine Bay K 8644. *J. Physiol.* **399:**559–575

Mc Donald, T.F., Pelzer, S., Trautwein, W., Pelzer, D. 1994. Regulation and modulation of calcium channels in cardiac, skeletal and smooth muscle cells. *Physiol. Rev.* **74:**365–507

Nocetti, F., Olcese, R., Qin, N., Zhou, J., Stefani, E. 1998. Effect of Bay K 8644 (−) and the $\beta_{2a}$ subunit on $Ca^{2+}$-dependent inactivation in $\alpha$1c $Ca^{2+}$ channels. *J. Gen. Physiol.* **111:**463–471

Reuter, H., Porzig, H., Kokubun, S., Prod'hom, B. 1988. Calcium channels in the heart. Properties and modulation by dihydropyridine enantiomers. *Ann. N. Y. Acad. Sci.* **522:**16–24

Sanguinetti, M.C., Kass, R.S. 1984. Voltage-dependent block of calcium channel current in the calf cardiac Purkinje fiber by dihydropyridine calcium channel antagonists. *Circ. Res.* **55:**336–348

Sanguinetti, M.C., Krafte, D.S., Kass, R.S. 1986. Bay K8644: Voltage-dependent modulation of Ca channel current in heart cells. *J. Gen. Physiol.* **88:**369–392

Shirokov, R., Levis, R., Shirokova, N., Ríos, E. 1992. Two classes of gating charge from L-type calcium channels in guinea pig ventricular cells. *J. Gen. Physiol.* **99:**863–895

Wei, X.Y., Rutledge, A., Triggle, D.J. 1989. Voltage-dependent binding of 1,4-dihydropyridine $Ca^{2+}$ channel antagonist and activators in cultured neonatal rat ventricular myocytes. *Mol. Pharmacology* **35:**541–552

## Appendix

The four-states model proposed by Brum et al. (1988) for the voltage sensor of excitation contraction coupling of the skeletal muscle of the frog has been also used to reproduce some of the properties of the cardiac L-type Ca channel by Shirokov et al. (1992). This basic model (Scheme 1) consists of four states: closed ($C$), open ($O$) (admittedly an oversimplification as there is evidence for more than one closed state and the maximum $P_o$ of Ca channels is ~0.1 when all the activating charge has moved, a property not reproduced by this simple model), and two inactivated states ($I_o$ and $I_c$) connected in a ring. The transitions between closed and open states and between inactivated states (horizontal transitions) are intrinsically voltage-dependent and generate charge 1 and charge 2, respectively. The transitions between available and inactivated states (vertical transitions) are assumed voltage-independent. An extension of this model assuming binding of DHP to all four states yields the eight-states model depicted in Scheme 2.

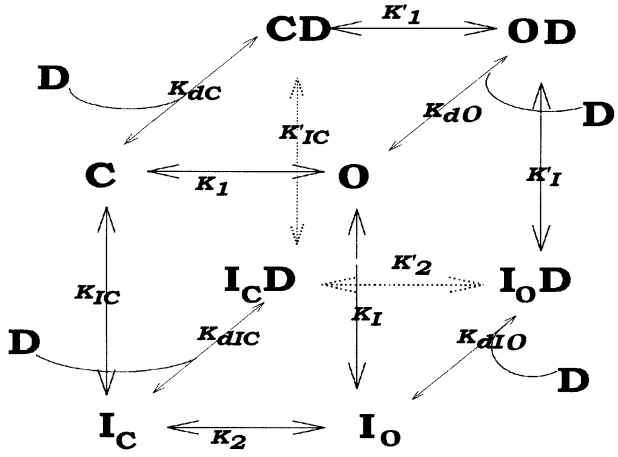


**Scheme 2.**

Drug bound states are indicated by adding a $D$ to the notation. The equilibrium constants between states are defined as follows:

$$K_1 = O/C, K_2 = I_O/I_C, K_I = I_O/O, K_{IC} = I_C/C$$

$$K'_1 = OD/CD, K'_2 = I_O D/I_C D,$$
$$K'_I = I_O D/OD, K'^{I}_{C} = I_C D/CD$$

The equilibrium between drug-free and drug-bound states is characterized by dissociation constants defined as $K_{dO} = O\,[D]/OD$, $K_{dC} = C[D]/CD$, $K_{d1O} = I_O\,[D]/I_O D$, $K_{d1C} = I_C\,[D]/I_C D$, where $[D]$ is the DHP concentration.

Following Brum et al. (1988) $K_1 = \exp\{(V-V_1)/k\}$, $K_2 = \exp\{(V-V_2)/k\}$, $K'_1 = \exp\{(V-V'_1)/k\}$, $K'_2 = \exp\{(V-V'_2)/k\}$, where $V_1$ and $V_2$ are the half-distribution voltages for charge 1 and charge 2, respectively, in the drug-free form, and $V'_1$ and $V'_2$ in the drug-bound form. $k$ is the e-fold voltage sensitivity, assumed to be the same for all the voltage-dependent steps. All these parameters of the model can be experimentally determined by the corresponding measurements in drug-free conditions and in the presence of saturating drug concentration.

As demonstrated by Brum et al. (1988), the four-state model steady-state availability curve is a Boltzmann function plus a constant. Its half distribution voltage, $V_{1/2}$, is given by

$$V_{1/2}/k = \ln[(\exp\{V_1/k\} + K_I \exp\{V_2/k\})/(1 + K^I)] \qquad \text{(A1)}$$

where $k$, the slope factor, has the same value as for $Q1$ and $Q2$ distributions. This equation is a reliable way to determine $K_1$, which can also be obtained as the ratio between the fraction of the total charge that inactivates and the fraction of the total charge that resists inactivation, provided that both measurements originate in the same set of channels.

The fourth equilibrium constant is not independent and is fixed by microscopic reversibility.

Similarly, the parameters for the drug-bound states were estimated in the presence of saturating drug concentration.

$$V'_{1/2}/k = \ln[(\exp\{V'_1/k\} + K'_I \exp\{V'_2/k\})/(1 + K'^{I})] \qquad \text{(A2)}$$

As microscopic reversibility applies to every possible cycle in the model, the twelve equilibrium constants are determined by five independent equations and only seven independent constants. As mentioned above, six of them were experimentally determined from the charge distributions and steady-state availability curves while the seventh is constrained by the dose-response curve. For instance,

$$(i) \quad K_{IC} = K_1 K_I / K_2$$

(*ii*) $K'_{IC} = K'_I K'_I / K'_2$

(*iii*) $K_{dO} = K_{dIO} K'_I / K_I$

(*iv*) $K_{dIC} = K_{dIO} K'_2 / K_2$

(*v*) $K_{dC} = K_{dO} K'_1 / K_1$

Some general conclusions can be drawn, from (*v*) $K_{dO}/K_{dC} = K_I/K'_I = \exp\{(V'_1 - V_1)/k\} < 1$ since $V'_1 < V_1$ therefore, the dissociation constant of the open state is smaller than that of the closed state. From (*iv*) since $K'_2/K_2 = 1$, based on the lack of change of the half distribution voltage of *Q2* upon drug application, the drug should bind to both inactivated states with equal affinity. Finally from (*iii*) it is concluded that $K_{dO}/K_{d1O} > 1$, since $K'_1/K_1 > 1$, given the more negative mid-voltage of the availability curve of the drug-bound form. Thus, the inactivated states have higher affinity for the drug, consistent with the promotion of inactivation by agonist drugs.

To simulate the experimental data with the agonist Bay K we chose the following values for the constants: $V_1 = 3$ mV, $V'_1 = -5$ mV, $V_2 = V'_2 = -90$ mV, $K_1 = 1.5, K'_1 = 4$, $K_{dO} = 20$ nM. The chosen value for $K_{dO}$ is equal to the $K_{0.5}$ value obtained by Lacerda and Brown (1989) for S(−)Bay K in their study of tail currents in ventricular myocytes. With the values used, above calculations based on microscopic reversibility yield $K_{dI} = 8$ nM and $K_{dC} = 34$ nM. The outcome of such simulations, as shown in Fig. 7. *A*, *B*, *C*, were calculated at 250 nM Bay K, a condition in which all the channels are in the drug-bound form, at the $V_h$ indicated in the figure. In *D*, the dose-response curve was calculated at $V_h = -40$ mV and the parameters plotted, $\Delta Q_{1max}$ and $\Delta V_1$, were obtained by fitting a Boltzmann function to the simulated data. This rather simple model successfully reproduces the stationary data, suggesting the plausibility of modulated receptor binding of DHP to the L-type channel.

From (A1), (A2), (*iii*), (*iv*) and (*v*) it follows that the shift in the mid point of the steady-state availability curve, $\Delta V_{1/2} = V'_{1/2} - V_{1/2}$, is given by:

$$\Delta V_{1/2} = k \ln \frac{[(K_{dO}/K_{dC})\exp(V_1/k) + (K_I K_{dO}/K_{dI})(\exp(V_2/k)](1 + K_I)}{[\exp(V_1/k) + K_I \exp(V_2/k)](1 + K_I K_{dO}/K_{dI})} \quad \text{(A3)}$$

Equation A3 expresses the contribution of drug binding to the different states to the overall effect on the availability curve. On this basis the statement that promotion of the open state will only shift $V_{1/2}$ by the same amount as $V_1$ can be put in quantitatively. If this is the case, as in Sanguinetti et al. (1986), $K_I$ is the same for both drug-free and drug-bound forms and $K_{dI} = K_{dO}$. Thus $\Delta V_{1/2} = k \ln (K_{dO}/K_{dC})$, which is the shift in $V_1$.

This model is also able to reproduce the effects of the antagonist (*simulations not shown*), by setting −2 mV as the shift in the activation curve and most important, $K_{d0} = 10\ K_{dI}$, a requirement to account for the ~30% reduction in $QI_{max}$ from $V_h = -40$ mV and a shift of −25 mV in the availability curve.